

Surface Chemistry and Electron-Transfer Kinetics of Hydrogen-Modified Glassy Carbon Electrodes

Tzu-Chi Kuo and Richard L. McCreery*

Department of Chemistry, The Ohio State University, 100 West 18th Avenue, Columbus, Ohio 43210

Gas-phase modification of glassy carbon (GC) was investigated in an attempt to make a C–H-terminated surface that is resistant to oxidation. By using a hot filament technique, hydrogen radicals were generated from a flow of hydrogen gas, and then the radicals attacked glassy carbon electrode surfaces. The modified glassy carbon surfaces were characterized first by X-ray photoelectron spectroscopy, where the shape of the carbon 1s band shows a distribution of carbon oxidation states different from a fresh polished surface. The oxygen-to-carbon atomic ratio is low (<3%) and stays low in air for weeks. Hydrogen treatment had minor effects on Ru(NH₃)₆^{3+/2+} cyclic voltammetry but increased ΔE_p for Fe^{3+/2+} from 176 to 466 mV for a scan rate of 0.2 V/s. There is no significant difference in voltammetry at fresh polished glassy carbon surfaces or hydrogen-modified surfaces for dopamine, Fe(CN)₆^{3-/4-}, and ascorbic acid. Raman spectroscopy of modified surfaces shows a small decrease in carbon disorder compared to the fresh polished glassy carbon with both microscopic and macroscopic observations. All these observations are consistent with the etching of the GC followed by formation of a hydrogen-terminated carbon surface. We attribute the major decrease in electron-transfer rate for aquated Fe^{3+/2+} to the absence of catalytic carbonyl sites on the hydrogen modified carbon.

The variable level and distribution of oxygen-containing functional groups on carbon electrode surfaces leads to significant variability in electrochemical reactivity, adsorption, and stability.^{1–4} In addition, the propensity of sp² carbon to adsorb both polar and nonpolar impurities further complicates attempts to produce reproducible, well-defined carbon surfaces.⁵ The relationship between carbon surface condition and electrochemical behavior has been studied extensively, in particular with respect to heterogeneous electron-transfer kinetics and electroanalytical applications.^{3,4} Of particular relevance here are the observations that redox systems vary in the sensitivity of their kinetics to carbon

surface conditions and that certain redox systems are catalyzed by surface oxides.^{6–8} For example, the observed heterogeneous electron-transfer rate constant (k^0) for aquated Fe^{3+/2+} is ~3 orders of magnitude larger when the surface has a significant coverage of carbonyl groups.⁶

Since polishing and most chemical or electrochemical pre-treatments yield variable levels of oxides on carbon, alternatives have been considered to control surface composition. Vacuum heat treatment,⁹ Ar⁺ sputtering in UHV,⁷ and anaerobic polishing in alumina/cyclohexane slurries can produce low oxide surfaces, but the O/C ratio subsequently increases in air.⁶ Gas-phase modifications of glassy carbon (GC), including an rf plasma, have been used to increase the surface oxide coverage, but the oxygen is distributed among several different functional groups.^{10–13} Thus far, a stable GC surface with zero or known function group coverage has not been prepared except in UHV, and such surfaces do not appear to be air or water stable.

The development of doped diamond films as electrode materials^{14–20} has resulted in a new approach to the problem, based on CVD techniques. A CH₄/H₂ plasma produces a diamond thin film on various substrates, including GC. If these films are doped to significant levels (~1%) with boron, they are conductive enough to act as electrodes. Swain introduced a modification to this approach which deleted the CH₄ and exposed GC to a H₂/H-atom microwave plasma.²¹ The resulting hydrogenated glassy carbon (HGC) surface appeared to have its carbon atoms terminated by C–H bonds, and HGC had electrochemical properties significantly

- (1) McCreery, R. L.; Cline, K. K.; McDermott, C. A.; McDermott, M. T. *Colloids Surf.* **1994**, *93*, 211.
- (2) Kinoshita, K. *Carbon: Electrochemical and Physicochemical Properties*; Wiley: New York, 1988.
- (3) McCreery, R. L. In *Electroanalytical Chemistry*; Bard, A. J., Ed.; Dekker: New York, 1991; Vol. 17, pp 221–374.
- (4) McCreery, R. L. In *Laboratory Techniques in Electroanalytical Chemistry*, 2nd ed.; Kissinger, P. T., Heineman, W. R., Eds.; Dekker: New York, 1996; Chapter 10.
- (5) Hu, I. F.; Karweik, D. H.; Kuwana, T. *J Electroanal Chem.* **1985**, *59*, 188.

- (6) Chen, P.; McCreery, R. L. *Anal. Chem.* **1996**, *68*, 3958.
- (7) Chen, P.; Fryling, M. A.; McCreery, R. L. *Anal. Chem.* **1995**, *67*, 3115.
- (8) McDermott, C. A.; Kneten, K. R.; McCreery, R. L. *J Electrochem. Soc.* **1993**, *140*, 2593.
- (9) Fagan, D. T.; Hu, I. F.; Kuwana, T. *Anal. Chem.* **1987**, *59*, 131.
- (10) Karweik, D.; Hu, I.-F.; Weng, S.; Kuwana, T. *ACS Symp. Ser.* **1985**, No. 288.
- (11) Evans, J. F.; Kuwana, T. *Anal. Chem.* **1979**, *51*, 358.
- (12) Miller, C. W.; Karweik, D. H.; Kuwana, T. *Anal. Chem.* **1981**, *53*, 2319.
- (13) Tse, D. C. S.; Kuwana, T. K. *Anal. Chem.* **1978**, *50*, 1315.
- (14) Xu, J.; Granger, M.; Chen, Q.; Strojek, J.; Lister, T.; Swain, G. *Anal. Chem.* **1997**, *69*, 590A.
- (15) Alehashem, S.; Chambers, F.; Strojek, J.; Swain, G.; Ramesham, R. *Anal. Chem.* **1995**, *67*, 2812.
- (16) Swain, G. M.; Ramesham, R. *Anal. Chem.* **1993**, *65*, 345.
- (17) DeClements, R.; Hirsche, B. L.; Granger, M.; Xu, J.; Swain, G. M. *J. Electrochem. Soc.* **1996**, *143*, L150.
- (18) Vinokur, N.; Miller, B.; Kalish, R. *J. Electrochem. Soc.* **1996**, *143*, L238.
- (19) Tenne, R.; Patel, K.; Hashimoto, K.; Fujishima, A. *J. Electroanal. Chem.* **1993**, *347*, 409.
- (20) Rueben, C.; Galun, E.; Cohen, H.; Tenne, R.; Kalish, R.; Hashimoto, Y.; Fujishima, A.; Butler, J. M. *J. Electroanal. Chem.* **1995**, *396*, 233.
- (21) DeClements, R.; Swain, G. M.; Dallas, T.; Holtz, M. W.; Merrick II, R.; Stickney, J. L. *Langmuir* **1996**, *12*, 6578.

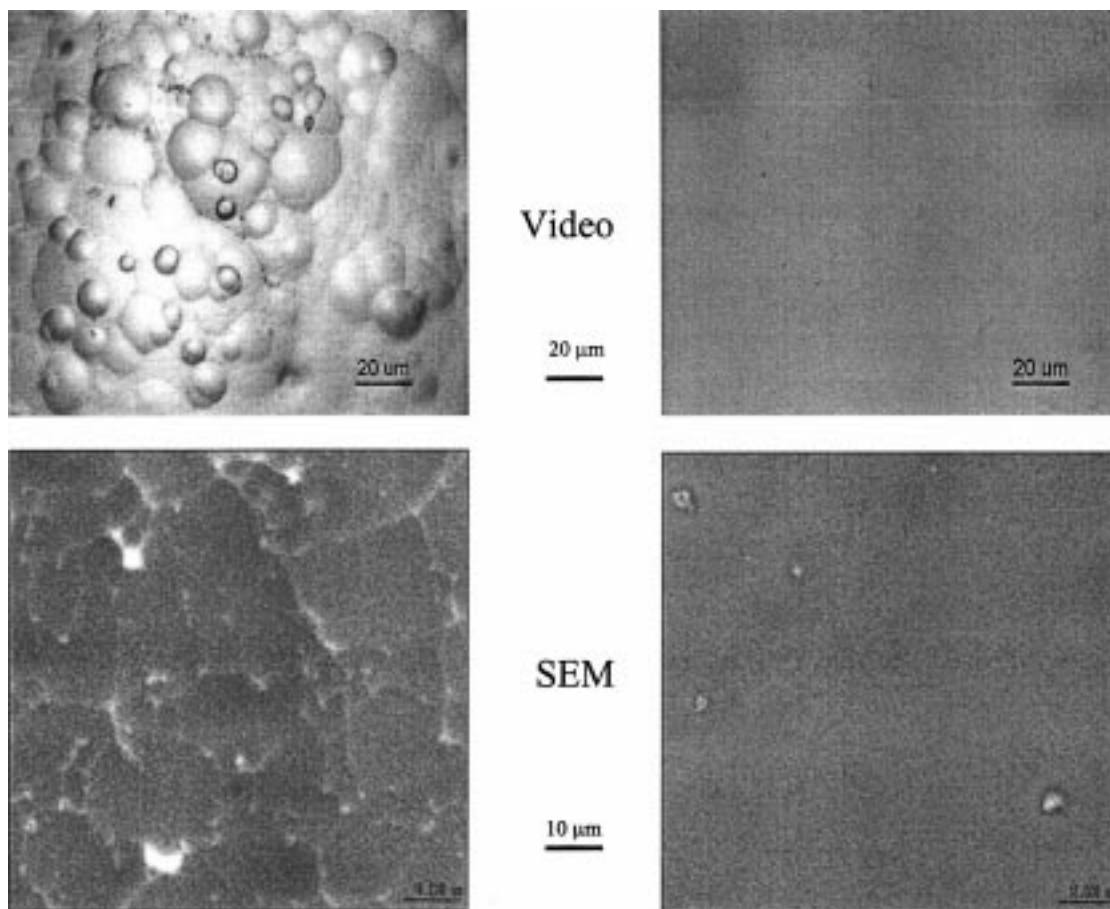


Figure 1. Bright-field optical (video) and SEM images of GC 20 before and after hydrogen treatment for 10 h. Right-hand micrographs are the polished surface, left-hand are following hydrogenation.

different from that of polished GC. HGC has low oxide coverage and low voltammetric background and maintains electron-transfer reactivity during prolonged exposure to laboratory air.

In the current report, HGC electrodes prepared by a hot filament method are compared to polished GC in terms of surface structure, stability, and electrode kinetics for several systems. Raman spectroscopy, XPS, and cyclic voltammetry reveal some important effects of hydrogen termination which may have substantial fundamental and electroanalytical value.

EXPERIMENTAL SECTION

Tokai GC-20 plates were used in this work for both hydrogen radical treatment and the control experiments. GC samples were polished as described elsewhere⁶ with Nanopure water/alumina slurries by hand, rinsed, and sonicated in water (Barnstead, Nanopure water) several times prior to hydrogen treatment. The sample was then placed on a sample holder inside a T-cell made of stainless steel, with a thermocouple tip in the center of the sample holder to monitor the sample temperature. The T-cell had a gas inlet at the top, ~4 cm above the sample holder, and the gas outlet was 7 cm below the sample holder to make sure the reaction gas hit the sample. A heating wire, made of tungsten and connected with an electric power feedthrough, was placed ~2 mm above the sample to provide the heat for the dissociation of hydrogen molecules.

After pumping down this cell to under 1×10^{-3} Torr, hydrogen gas was introduced into the system with a typical flow rate at 99.8

scm. Then the filament was turned on and heated the sample slowly to 600 °C, while the W wire itself rose to ~2000 °C. The system pressure was ~35 Torr and changed slightly with temperature during the treatment. The samples stayed at 600 °C for times ranging from 6 to 10 h, and then the filament was turned down slowly and turned off. Hydrogen gas was kept flowing for another 30 min before the sample was taken out.

The bimolecular rate constant for the reaction of $2\text{H}_2 \rightarrow 2\text{H} + \text{H}_2$ is $5.8 \times 10^{-19} \text{ cm}^3 \text{ molecule}^{-1} \text{ s}^{-1}$ at 2000 °C,²² so the rate of the production of hydrogen radical was $\sim 2.6 \times 10^{16} \text{ radical cm}^{-3} \text{ s}^{-1}$ with a concentration $1.5 \times 10^{17} \text{ molecule cm}^{-3} \text{ H}_2$. The estimated flow velocity of gas was 11 cm/s near the glassy carbon surface.

X-ray photoelectron spectra were acquired with a VG Scientific Escalab MKII spectrometer with a Mg X-ray source. All photoelectron spectra were taken with a pressure of less than 2×10^{-9} Torr. Both survey and high-resolution spectra for C and O 1s were collected, and the O/C atomic ratio was obtained by integrating the area under the peaks, followed by correction with their sensitivity factors.

Raman spectra were taken with two different systems. The macroscopic Raman spectra were taken on a *f*/4 spectrograph (Chromex IS250) with a 1200 groove/mm grating and a 1152 × 384 CCD maintained at -110 °C. Scattering was collected by a *f*/1.4 camera lens in front of the sample with 180° optical geometry

(22) Cohen, N.; Westberg, K. R. *J. Phys. Chem. Ref. Data* **1983**, *12*, 531.

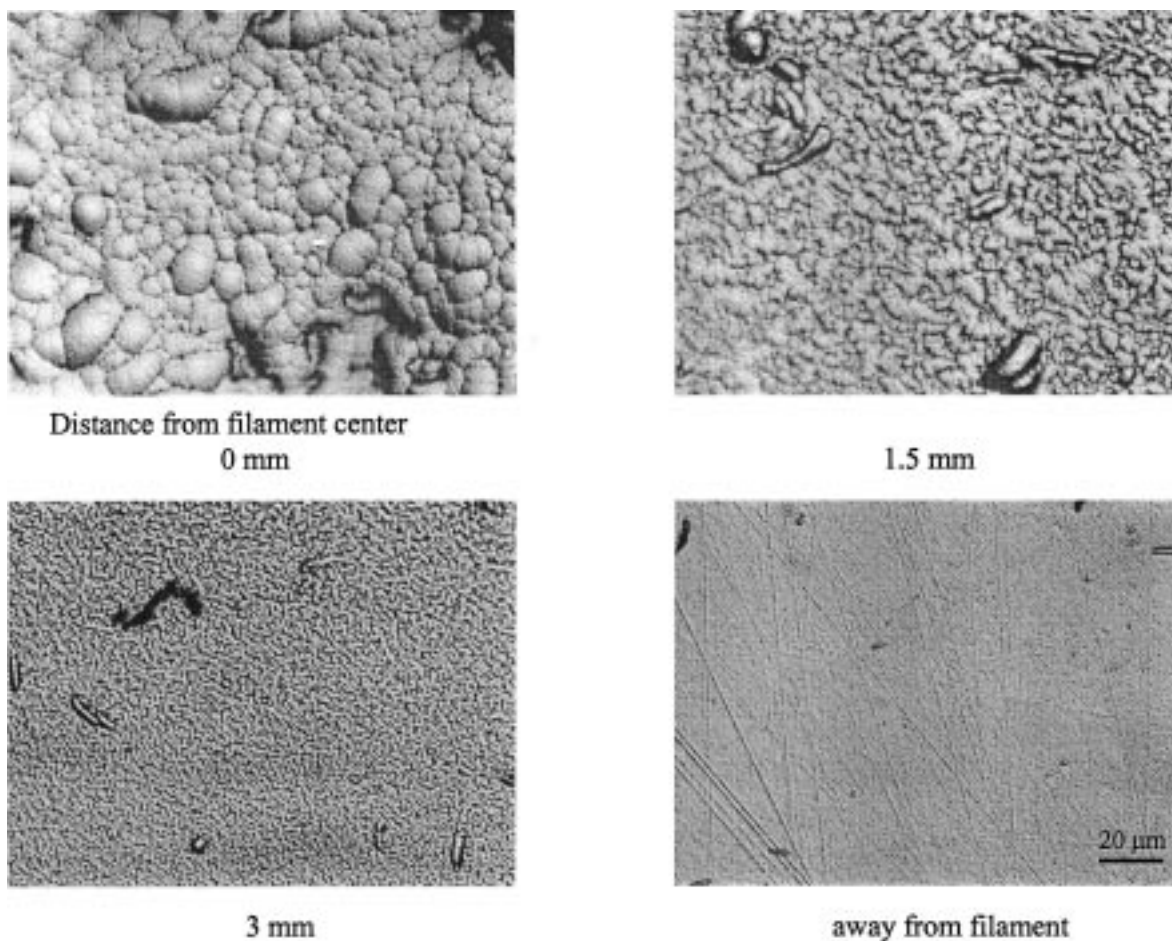


Figure 2. Bright-field optical micrographs of an HGC surface treated for 20 min, at varying distances from the center of the hot filament. The scale is the same for all images.

and then filtered by a band rejection filter followed with a $f/4$ lens before entering the spectrograph.²³ Microscopic Raman spectra were obtained on a Dilor X - Y system with a 2000×800 front-illuminated CCD maintained at -133 °C. A band rejection filter was placed before the entrance slit to a single spectrograph that was equipped with a 1200 or 1800 groove/mm grating.²⁴ A $50\times$ objective was used in most cases. The excitation source for both systems was 514.5-nm line from an Ar^+ laser (Coherent, Innova 300).

Cyclic voltammetry was performed with a computer-controlled potentiostat (Bioanalytical System, BAS, model 100). A BAS Ag/AgCl (3 M NaCl) reference electrode and a platinum auxiliary electrode were used. The glassy carbon plate was put into a Teflon cell with an O-ring seal to maintain the insulation of wires; all solutions were prepared daily prior to use, and all solutions were saturated with argon gas for at least 20 min prior to cyclic voltammetry. The GC samples were sonicated in Nanopure water after being polished in Al_2O_3 slurries. Isopropyl alcohol (IPA) containing activated carbon powder (3:1 by volume) was employed as indicated to remove contamination on samples. Following 2-propanol treatment, samples were sonicated in Nanopure water immediately.

To distinguish the difference between exposing the surface to hydrogen radicals and to air, we studied the change on ET

kinetics of polished glassy carbon surfaces with air exposure and different ways of cleaning surfaces. There were four steps before cyclic voltammetry was carried out after each step in the following order: fresh polished (step I); 10 hours in air after step I (step II); sonication in Nanopure water (step III); and then sonication in isopropyl alcohol and activated carbon powder, followed by Nanopure water (step IV). The samples were rinsed thoroughly with Nanopure water after step I in order to remove residuals from the voltammetry solution, then were dried with Ar flow, and put in air for 10 h for step II, where a 10-h duration was chosen for simulation of the hydrogen treatment duration.

The redox systems and chemicals used in this work were as follows: 1 mM Fe^{2+} in 0.2 M HClO_4 made from $\text{Fe}(\text{NH}_4)_2(\text{SO}_4)_2 \cdot 6\text{H}_2\text{O}$ (Mallinckrodt, Inc.) and 70% HClO_4 (GFS chemicals); $\text{Ru}(\text{NH}_3)_6^{3+}$ in 1 M KCl solution made from $\text{Ru}(\text{NH}_3)_6\text{Cl}_3$ (Strem Chemicals); 1 mM $\text{Fe}(\text{CN})_6^{4-}$ in 1 M KCl solution made from $\text{K}_4\text{Fe}(\text{CN})_6$ (J. T. Baker); 1 mM dopamine (Sigma) in 0.1 M phosphate buffer solution at pH 7; 1 mM ascorbic acid (AA, Aldrich Chemical Co.) in 0.1 M H_2SO_4 solution.

The nitrophenyl derivatization was carried out with 1 mM 4-nitrobenzenediazonium tetrafluoroborate (97%, Aldrich) in acetonitrile (99.9%, Mallinckrodt).

RESULTS AND DISCUSSION

Morphology and Raman. The microscopic bright-field image of hydrogen-treated GC exhibits nodular structures of variable diameter (Figure 1), while there are no observable features at

(23) Ray, K. G.; McCreery, R. L. *Appl. Spectrosc.* **1997**, *51*, 108–116.

(24) Ray, K. G.; McCreery, R. L. *Anal. Chem.* **1997**, *69*, 4680–4687.

Table 1. Raman Results for Various GC Surfaces

	HGC	0.05- μm Al ₂ O ₃ polished GC	1- μm Al ₂ O ₃ polished GC	14.5- μm grit paper polished GC
D/E _{2g} band area ratio	1.54 \pm 0.04 ^a (N = 6) ^b	1.86 \pm 0.01 (N = 3)	1.81 \pm 0.03 (N = 3)	1.50 \pm 0.02 (N = 3)
fwhm of D band (cm ⁻¹)	50.1 \pm 1.9	56.3 \pm 0.1	58.8 \pm 0.2	79.1 \pm 0.8
fwhm of E _{2g} band (cm ⁻¹)	65.1 \pm 2.0	71.5 \pm 0.4	73.4 \pm 0.7	95.3 \pm 0.4

^a Mean \pm standard deviation. ^b N is number of surfaces examined.

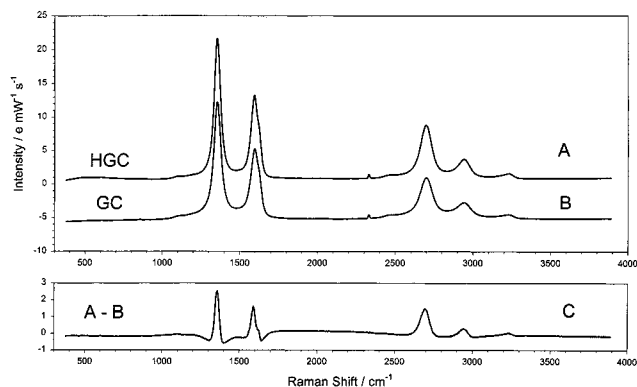


Figure 3. Raman spectra of GC and HGC, with a 514.5-nm laser. Small peak at 2331 cm⁻¹ is atmospheric nitrogen. Lower spectrum is the GC spectrum subtracted from that of HGC.

the same magnification on a fresh polished GC surface before the treatment. The scanning electron microscopy images show the details of these surfaces at higher magnification. The polished GC surface still appears smooth with only some inherent pits, presumably from gas bubbles remaining in the bulk material during the fabrication of GC, which were then exposed by polishing. The HGC surface, on the other hand, exhibits morphological features ranging from 1 μm to tens of micrometers in size. The thickness of glassy carbon plates decreased with treatment duration in the hydrogen plasma. Figure 2 shows videomicrographs of a GC surface treated for 20 min in the hydrogen plasma, at various positions relative to the hot filament. As the imaged area progresses toward the center of the filament, the roughness increases but remains uniform over the field of view. The results imply that the H-atom plasma is etching the GC surface, removing both polishing debris and bulk GC material. The nodules observed on HGC are similar to those reported by Swain et al. but are larger than those observed for fractured GC by SEM²⁵ and STM.²⁶

Raman spectra of HGC shown in Figure 3 are qualitatively similar to that for polished GC-20, with no apparent additional peaks. Possible C-H vibrations would be expected in the 2800–3100-cm⁻¹ region but would be weak. At best, the C-H bonds would be present as a monolayer, and their Raman scattering is apparently obscured by second-order features from the ~ 250 Å of GC sampled by the spectrometer. Subtraction of the HGC from polished GC spectra reveals a residual that is due to a change in line width during hydrogen treatment. This change is apparent in Table 1, which lists line widths and peak area ratios for the D and E_{2g} bands of various surfaces. The D/E_{2g} ratio is an indication

(25) Rice, R. Ph.D. Dissertation, The Ohio State University, Columbus, OH, 1990.

(26) McDermott, M. T.; McDermott, C. A.; McCreery, R. L. *Anal. Chem.* **1993**, *65*, 937.

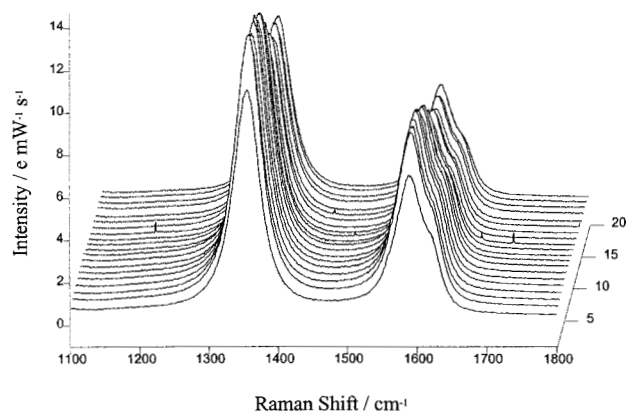
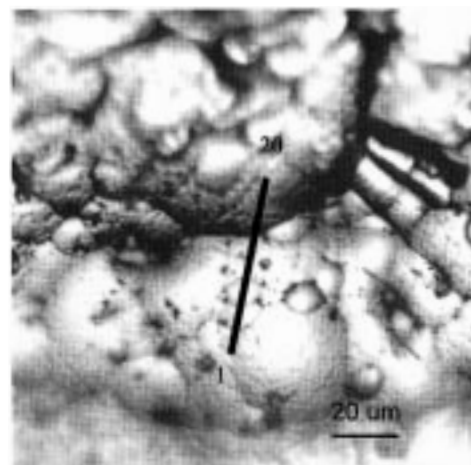


Figure 4. Twenty Raman spectra obtained from ~ 2 - μm circular areas along the line shown in the optical micrograph of HGC. Intensity is in terms of photoelectrons divided by laser power and integration time.

of disorder, with the larger value on polished GC indicating a more disordered material than either HGC or fractured GC.³ As reported earlier, polishing leads to an increase in this ratio due to mechanical disordering of the GC structure.²⁷ Apparently, the hydrogen etching has removed this disordered layer and reduced the D/E_{2g} ratio to a value similar to the fractured surface. It is likely that fractured GC reflects the bulk disorder of GC, implying that hydrogen etching has exposed the bulk GC material.

The uneven morphology of the HGC surface raises the question of structural heterogeneity in the GC surface after modification. A Raman microprobe (50 \times objective, ~ 2 - μm spot size) was used to observe changes in D/E_{2g} ratio across the HGC surface. Figure 4 shows 20 spectra obtained along the line indicated in the videomicrograph. Although the Raman intensity

(27) Rice, R.; Allred, C.; McCreery, R. L. *J. Electroanal. Chem.* **1989**, *263*, 163.

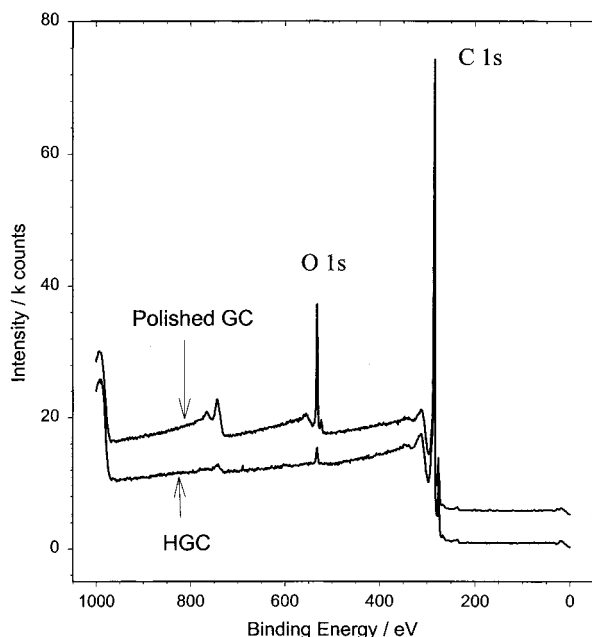


Figure 5. Survey XPS spectra of polished GC (upper) and HGC (lower) immediately after hydrogenation.

varies along the line due to changes in focus from the rough surface, the D/E_{2g} ratio for the 20 spectra is 1.40 ± 0.031 (2.2%). The standard deviation is comparable to the 4–6% RSD observed for fractured or polished GC.²⁴

X-ray Photoelectron Spectroscopy. All hydrogen-treated glassy carbon surfaces were examined with X-ray photoelectron spectroscopy immediately after modification prior to any other measurements. A survey XPS spectrum of a typical hydrogen-treated sample is compared to one from polished GC in Figure 5. Freshly polished glassy carbon has an O/C atomic ratio ranging from 8 to 15%, but this value decreased to 1–4% after hydrogen treatment.

Figure 6 shows high-resolution XPS spectra of the C_{1s} region for several surfaces. The polished GC sample exhibits a shoulder in the region of 286.5–288 eV, which is commonly attributed to carbon atoms associated with surface oxides. Hydrogen treatment reduces this shoulder to essentially undetectable levels, consistent with the decrease in the O_{1s} peak. When the O/C ratio is monitored as a function of air exposure time (Figure 7), the ratio for polished GC stays constant for at least 10 days. In contrast, the O/C for VHT or cyclohexane/alumina-polished GC starts low but increases over a several-day period. The hydrogenated surface remains less than 2% after 2 weeks of air exposure, but does slowly increase to 4% after 40 days in air.

Voltammetric scans in 0.2 M $HClO_4$ increased the O/C ratio of HGC, with the amount depending on the positive potential limit. Table 2 lists XPS O/C ratios for an HGC sample after various potential excursions. When the positive potential limit was increased from +1.0 to +1.5 V vs Ag/AgCl, the O/C ratio increased significantly.

Electron-Transfer Kinetics. To examine the effect of hydrogen treatment on electrode kinetics, five common redox systems were selected, on the basis of their sensitivity to surface chemistry.⁶ Of interest are the magnitude and stability of k^o values for these systems on HGC, compared to polished GC. $Ru(NH_3)_6^{3+/2+}$

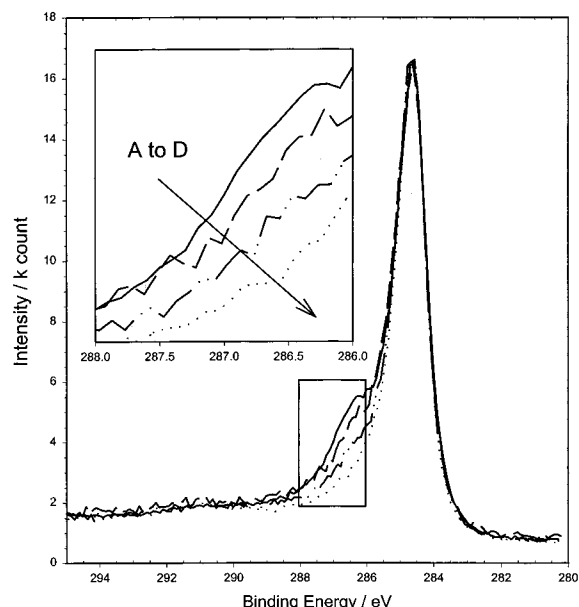


Figure 6. High-resolution XPS of C 1s region for several GC surfaces, with shoulder region expanded in the inset. A, polished GC; B, HGC after cyclic voltammetry in 0.2 M $HClO_4$; C, surface B after cleaning with 2-propanol/activated carbon; D, freshly prepared HGC.

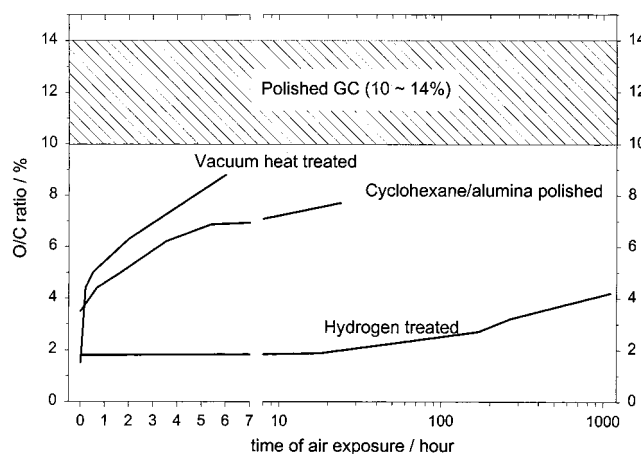


Figure 7. O/C atomic ratio from XPS as a function of air exposure for four GC surfaces. Except for the duration of the XPS measurement itself, the surfaces remained in laboratory air. Polished GC surface had varying O/C from 10 to 14%, but stayed constant in air. Note discontinuity in x-axis to show long exposure times.

has been shown to be insensitive to surface oxides or monolayer films and acts as an indicator of thick films or insulators. $Fe_{aq}^{3+/2+}$ has been shown to be catalyzed by surface carbonyl groups and, therefore, observed k^o values quite sensitive to surface oxidation.^{6,28} $Fe(CN)_6^{3-/4-}$, ascorbic acid, and dopamine exhibit fast kinetics on GC with low oxide coverage but are decelerated when an adventitious or intentional monolayer is present.⁶ Voltammograms of these systems were obtained for polished GC and HGC before and after 10 h of exposure to laboratory air followed by water or IPA sonication as described in the Experimental Section.

Raw voltammograms (without background subtraction) for dopamine at pH 7 are shown in Figure 8 to illustrate the effects of electrode material. Notice that ΔE_p for HGC is similar to that

(28) McDermott, C. A.; Kneten, K. R.; McCreery, R. L. *J. Electrochem. Soc.* **1993**, *140*, 2593.

Table 2. Oxygen Coverage and Voltammetric Results for HGC

	O/C ratio from XPS (%)	ΔE_p for $\text{Fe}^{3+/2+}$, 0.2 V/s, mV	k^0 for $\text{Fe}^{3+/2+}$, cm/s
immediately after hydrogen plasma	3.6		
first cycle 0 to +1.0 V		586	4.0×10^{-5}
after 20 cycles, 0 to +1.0 V	5.6	526	7.2×10^{-5}
after 22 additional cycles, -0.5 to 1.0 V	6.2	465	1.3×10^{-4}
22 additional cycles, -0.5 to 1.5 V	11.0	280	7.8×10^{-4}
120 additional cycles, -0.5 to 1.5 V	14.2	128	4.6×10^{-3}

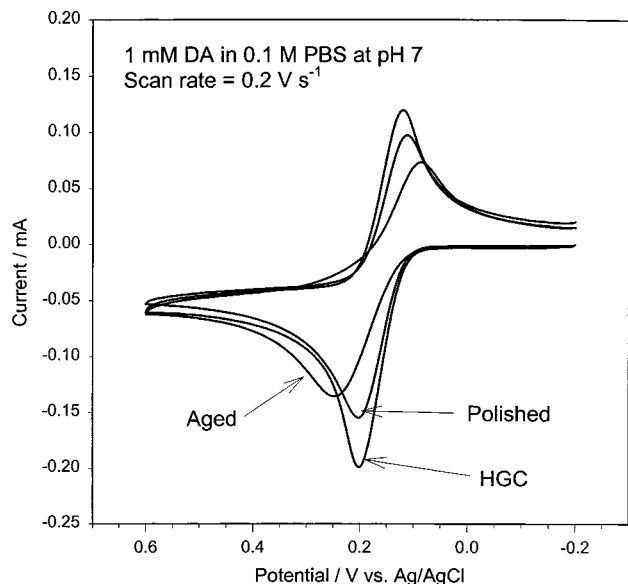


Figure 8. Cyclic voltammograms for dopamine (DA) on polished GC, HGC, and polished GC aged for 10 h in laboratory air. PBS, phosphate buffered saline, pH 7.

for a polished GC surface. Kinetic results for $\text{Fe}^{3+/2+}$, $\text{Ru}(\text{NH}_3)_6^{3+/2+}$, $\text{Fe}(\text{CN})_6^{3-/4-}$, dopamine, and AA are listed in Tables 2 and 3. $\text{Fe}^{3+/2+}$ was quite sensitive to the surface O/C ratio, and its ΔE_p decreased with potential cycling as the O/C ratio increased. (Table 2)

Surface Modification. Modification of the HGC with a monolayer of nitrophenyl groups was attempted, to assess the reactivity of HGC to phenyl radicals. Reduction of nitrophenyldiazonium ion in acetonitrile at polished GC or graphite electrodes yields a compact nitrophenyl monolayer observable with XPS, Raman, and voltammetry.²⁹ The same procedure was applied to HGC electrodes, resulting in the voltammograms and Raman spectra of Figures 9 and 10. The voltammogram on GC is typical for diazonium reduction, with a rapid decrease in current with successive scans as the monolayer is formed. On HGC, the first scan is quite different, while the second, third, fourth scans follow a trend similar to that for polished GC. The Raman spectra of GC and HGC after nitrophenyl derivatization are quite similar, exhibiting prominent 849- and 1108–1177- cm^{-1} bands corresponding to the NO_2 and phenyl C–H bending motions, similar to those reported previously for GC.²⁹

Contact Angle. The static contact angle for water on GC and HGC surfaces was observed after a variety of surface treatments, with the results listed in Table 4. Air exposure causes an increase in contact angle, presumably due to hydrocarbon impurity adsorption. For GC, the 2-propanol/activated carbon cleaning reduces the contact angle to values lower than the fresh polished case. HGC exhibits a higher contact angle than GC, but this value is reduced significantly by electrochemical oxidation, particularly with a maximum potential of +1.5 V vs Ag/AgCl.

DISCUSSION

The microscopy, XPS, and Raman results from polished GC and HGC are consistent with H-atom etching of the GC surface followed by (or coincident with) formation of surface C–H bonds. The major reduction in surface O/C during hydrogenation indicates removal of surface oxides. While direct observation of C–H bonds is not possible with XPS, we infer that surface oxygen groups are replaced by hydrogen atoms, as C–H bonds. The D/ E_{2g} ratio from Raman spectroscopy indicates that HGC is somewhat more ordered than polished GC, presumably due to removal of surface layers which had been mechanically disturbed by polishing. In fact, the D/ E_{2g} ratio for HGC is similar to that for fractured GC (Table 1), implying that both have a bulk GC microstructure over the 250-Å depth sampled by the Raman measurement.³⁰ On the basis of an estimated Raman cross section for a surface C–H vibration, it would be difficult to observe such features above the background scattering from second-order phonons.

In contrast to the other low-oxide GC surfaces examined, the O/C ratio on HGC remains low upon prolonged exposure to laboratory air. It is well-known that dioxygen at room temperature does not react with basal plane graphite but does react with edge sites.³¹ A common premise involves a radical–radical reaction between O_2 and an unsatisfied radical site on the edge plane. For the case of VHT and cyclohexane/ Al_2O_3 -polished GC, many radical sites would be expected to remain after pretreatment, which are free to react with O_2 . Based on Figure 7, this reaction is fairly slow in ambient air but does increase the O/C ratio from ~ 2 to $\sim 7\%$ in several hours. For HGC, however, surface radical sites are likely to be occupied by H-atoms as C–H bonds and are unavailable for reaction with O_2 . This C–H termination of the carbon edges leads to the long-term stability of the surface toward air oxidation exhibited in Figure 7. However, C–H termination does not appear to prevent electrochemical surface oxidation in 0.2 M HClO_4 in water. Potential excursions to +1.0 V vs Ag/AgCl cause some increase in the O/C ratio, but a sharper increase occurs at 1.5 V (Table 2). Not surprisingly, the magnitude of the increase in O/C ratio depends on both the magnitude and duration of the positive potential.

Although the contact angle observations (Table 4) are difficult to interpret quantitatively due to surface roughness and adventitious impurities, the trends are consistent with XPS and kinetic observations. Polished GC becomes more hydrophobic with air exposure, presumably due to adsorption of hydrocarbons or similar hydrophobic impurities. 2-Propanol appears to remove such adsorbates and return the contact angle to a value lower than that

(29) Liu, Y.-C.; McCreery, R. L. *J. Am. Chem. Soc.* **1995**, *117*, 11254.

(30) Alsmeyer, Y. W.; McCreery, R. L. *Anal. Chem.* **1991**, *63*, 1289.

(31) Chang, H.; Bard, A. J. *J. Am. Chem. Soc.* **1991**, *113*, 5588.

Table 3. ΔE_p (mV) of Five Redox Systems on Different GC Surfaces

	step 1 fresh polished GC	step 2 polished GC in air 10 h	step 3 water sonicated	step 4 solvent and water cleaning	HGC	HGC in air 10 h	HGC after solvent and water cleaning
Ru(NH ₃) ₆ ^{3+/2+} (+0.2 to -0.6 V) ^a	120 ± 4 ^b (0.040 ± 0.003) ^c	114 ± 2 (0.045 ± 0.002)	113 ± 1 (0.046 ± 0.001)	122 ± 2 (0.039 ± 0.001)	120 ± 5 (0.040 ± 0.004)	124 (0.038)	120 ± 3 (0.040 ± 0.002)
Fe ^{3+/2+} _{aq} (0 to 1 V)	176 ± 4 (2.36 ± 0.11) × 10 ⁻³	425 ± 12 (1.91 ± 0.22) × 10 ⁻⁴	477 ± 19 (1.16 ± 0.21) × 10 ⁻⁴	267 ± 6 (8.89 ± 0.53) × 10 ⁻⁴	466 ± 29 (1.28 ± 0.36) × 10 ⁻⁴		341 ± 28 (4.3 ± 1.1) × 10 ⁻⁴
Fe(CN) ₆ ^{3-/4-} (-0.2 to +0.8 V)	135 ± 7 (0.037 ± 0.004)	154 ± 6 (0.028 ± 0.002)	148 ± 7 (0.030 ± 0.003)	134 ± 8 (0.037 ± 0.005)	119 ± 5 (0.049 ± 0.005)		122 ± 3 (0.046 ± 0.003)
dopamine (-0.2 to +0.6 V)	87 ± 4	164 ± 7	150 ± 3	92 ± 4	91 ± 1	97	81 ± 4
ascorbic acid (E _{pa}) (0 to +0.9 V)	356 ± 4	392 ± 4	355 ± 1	317 ± 2	335	347	321

^a Potential scan range. ^b All values stated as mean ± standard deviation. ^c k^o , cm/s.

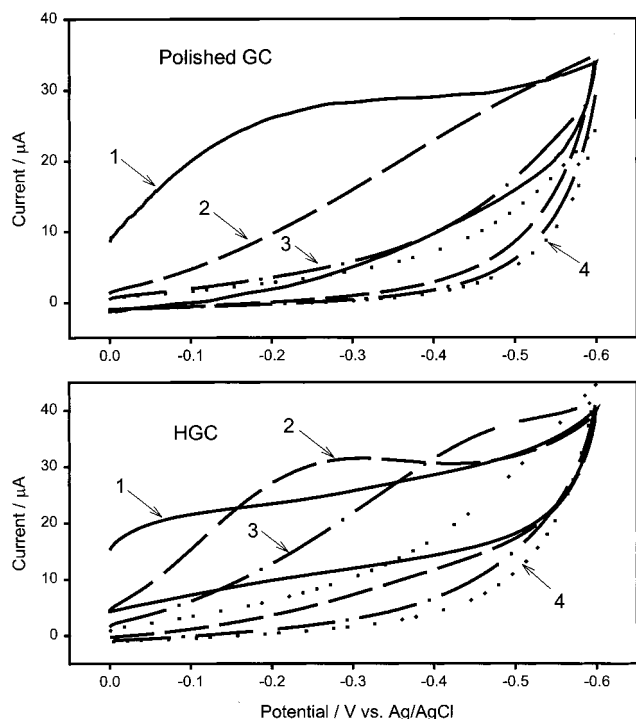


Figure 9. Voltammograms of nitrophenyldiazonium tetrafluoroborate in acetonitrile on polished GC and on HGC. Scan rate was 0.2 V/s. Numbers on curves indicate the order in which successive scans were acquired.

of the polished surface. HGC is more hydrophobic than polished GC, presumably due to the lack of surface oxides. Electrochemical oxidation makes the surface more hydrophilic, with a drastic reduction in contact angle after extended exposure to a potential of 1.5 V vs Ag/AgCl.

At first consideration, hydrogenation has minor effects on the kinetics of the five redox systems considered, except for Fe^{3+/2+}. These observations are best examined in the context of previously reported behavior of all five redox systems on carbon and metal electrodes.⁶ Ru(NH₃)₆^{3+/2+} is considered outer sphere, and the effects of surface impurities or oxides on its kinetics are minor. Even when an intentional monolayer is present on a GC surface, k^o for Ru(NH₃)₆^{3+/2+} is reduced only by an amount consistent with electron tunneling through the monolayer. As is apparent from Table 3, air exposure and subsequent water or IPA cleaning have minor effects on Ru(NH₃)₆^{3+/2+}, as does hydrogenation. As expected, C-H termination does not and should not inhibit outer-

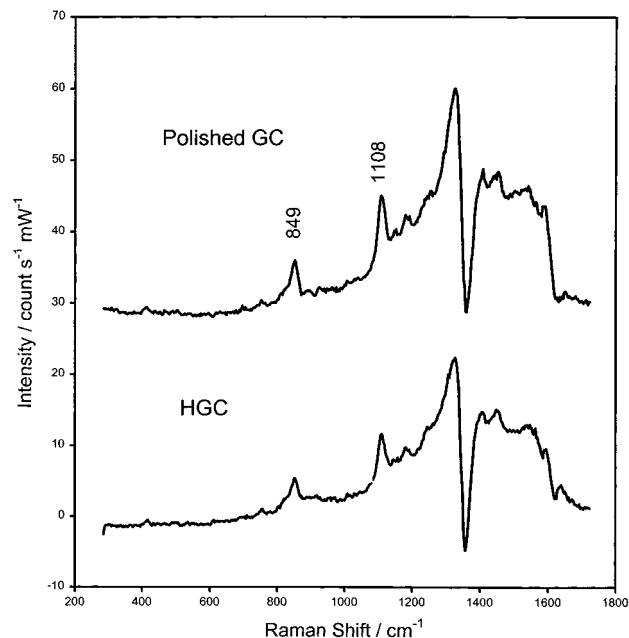


Figure 10. Raman spectra of HGC and polished GC following the voltammetric derivatization shown in Figure 9. Spectra of underivatized surface was subtracted. Integration time was 150 s; laser power at sample was 5 mW.

sphere electron transfer to Ru(NH₃)₆^{3+/2+}. Fe^{3+/2+} is a very different case, with a slow outer-sphere rate ($k^o \sim 10^{-5}$ cm/s) and a much faster electrocatalytic rate if carbonyl groups are present.⁶ Typical GC surfaces exhibit a k^o for Fe^{3+/2+} of $\sim 10^{-3}$ cm/s, due mainly to catalysis by the $\sim 1\%$ carbonyl coverage on polished GC. If the O/C ratio is very low, or if the surface is covered by a monolayer, k^o for Fe^{3+/2+} decreases to the outer-sphere rate of $\sim 10^{-5}$ cm/s. As expected, C-H termination yields a much slower k^o by removing C=O sites. When the HGC surface is oxidized electrochemically, the observed k^o for Fe^{3+/2+} increases, presumably because at least some of the oxides formed are surface carbonyl groups. As is apparent from Table 2, this effect becomes more pronounced when the maximum positive potential is increased from +1.0 to +1.5 V vs Ag/AgCl.

Fe(CN)₆^{4-/3-}, dopamine, and AA have been shown to exhibit fast electron transfer on low-oxide GC surfaces,^{6,9} implying that oxygen functional groups are not necessarily involved in electron transfer.⁶ However, these systems are slower on surfaces with intentional monolayers, implying some sort of surface interaction

Table 4. Static Contact Angle for Water on GC and HGC

	contact angle, deg
GC	
fresh polished	37–45
after 3 days in air	60
after 3 months in air	93
polished, after IPA and activated carbon	31–32
HGC	
fresh	65
after IPA and activated carbon	42
fresh, then 22 cycles, 0.0–1.0 V vs Ag/AgCl	57
after 22 additional cycles, –0.5 to +1.0 V	62
after 22 additional cycles, –0.5 to +1.5 V	30
after 120 cycles, –0.5 to +1.5 V	17

associated with electron transfer. Whatever this interaction, it is operative on the HGC surface. $\text{Fe}(\text{CN})_6^{4-/3-}$, dopamine, and AA have slightly higher observed k^o values on HGC than on polished GC, for both initial and IPA-treated surfaces. IPA cleaning of either GC or HGC results in an anodic peak potential for AA as low as those reported for very effective activation procedures such as laser activation and VHT. The slightly lower E_p on HGC compared to polished GC (335 vs 356 mV) may indicate a slightly cleaner HGC surface, since it is resistant to adsorption of whatever impurities cause the rate reduction on conventional surfaces.

The well-known properties of carbon as an adsorbent are significantly enhanced by the presence of surface oxides. Various mechanisms underlie this effect, including the creation of local dipoles, electrostatic attraction, and possible covalent bond formation with adsorbates. Oxide-free carbon can still adsorb many materials, but at reduced capacity. Speaking generally, polar adsorbates interact more strongly with oxidized surfaces, but nonpolar materials usually adsorb through induced dipole and van der Waals interactions. As proposed by DeClements et al.,²¹ the long-term stability of diamond and HGC may be due to weaker adsorption of polar adventitious impurities, which may decelerate electron-transfer reactions. This hypothesis is supported by the data of Table 3, particularly for $\text{Fe}^{3+/2+}$ and dopamine. Ten hours of air exposure significantly increases ΔE_p for $\text{Fe}^{3+/2+}$ and dopamine on polished GC, but sonication in 2-propanol restored much of the initial electron-transfer reactivity. At least for dopamine and ascorbic acid, the effect of air exposure on kinetics at HGC is much smaller.

The covalent bonding of nitrophenyl to GC upon reduction of the nitrophenyldiazonium ion is believed to occur via a nitrophenyl radical intermediate.^{33,34} This radical can attack both basal and edge carbon sites to lead to a compact monolayer. In the case of

HGC, the voltammetry implies a slower derivatization reaction, and the charge required for complete derivatization is greater than for GC. Since nitrophenyl radical cannot bind directly to C–H sites, it may be abstracting an H-atom to form a surface radical and soluble nitrobenzene. This surface radical then reacts with a second nitrophenyl radical to form the monolayer. The end result is the same as nitrophenyl derivatization of polished GC, but the initial voltammetric sweep is at least partly “wasted” to form solution-phase nitrobenzene. The electrode kinetic properties of the derivatized “HGC” are currently being compared to those of derivatized GC.

Although the current results do not provide direct proof for the existence of an H-terminated surface on HGC, all of the evidence is consistent with H-atom termination of radical or oxide sites. A C–H monolayer or submonolayer would not be expected to increase the tunneling distance for electron-transfer substantially; hence HGC and GC have comparable rate constants for $\text{Ru}(\text{NH}_3)_6^{3+/2+}$. The low O/C ratio of HGC accounts for the slow $\text{Fe}^{3+/2+}$ kinetics, due to the lack of carbonyl sites. However, potential excursions to +1.0 V or greater during voltammetry increase the O/C and the k^o for $\text{Fe}^{3+/2+}$. Although the HGC surface oxidizes in air very slowly, it does appear to oxidize at modest positive potentials in water. The long-term stability of HGC in air is attributed to significantly weaker adsorption to the H-terminated surface compared to GC and to its resistance to air oxidation. Surface oxides have long been known to increase adsorption to carbon, due to local electron withdrawal by oxygen, and the possibility of ionic and covalent bonding of adsorbates.

The HGC and GC results reported here are generally consistent with the observations of Swain et al. and Miller et al. for HGC²¹ and diamond^{14–20} electrodes, as well as the emerging understanding of factors affecting the electrochemical behavior of GC.^{1–4} The lack of oxides on HGC and diamond leads to stability and weak adsorption but also removes the catalytic sites important to certain redox systems such as $\text{Fe}^{3+/2+}$. HGC and boron-doped diamond have different electronic properties, but both can be conductive enough to support outer-sphere electron transfer. A significant difference between HGC and boron-doped diamond occurs for dopamine, which is quite slow on diamond but fast on HGC and GC. As is the case for outer-sphere systems and electrocatalytic $\text{Fe}^{3+/2+}$, detailed knowledge of the catechol/quinone redox mechanism is required to understand such differences. Once the nature of the interactions between dopamine and the surface are known, the origin of the differences among diamond, HGC, and GC should become clear.

ACKNOWLEDGMENT

The authors thank Professor Greg Swain for numerous useful conversations and Professor Vish Subramaniam for use of the hot filament apparatus. This work was supported by the National Science Foundation Analytical and Surface Chemistry Division.

Received for review July 13, 1998. Accepted February 1, 1999.

AC9807666

(32) Bansal, R. C.; Donnet, J.-B.; Stoeckli, F. *Active Carbon*; Dekker: New York, 1988.

(33) Allongue, P.; Delamar, M.; Desbat, B.; Fagebaume, O.; Hitmi, R.; Pinson, J.; Saveant, J.-M. *J. Am. Chem. Soc.* **1997**, *119*, 201.

(34) Delamar, M.; Hitmi, R.; Pinson, J.; Saveant, J.-M. *J. Am. Chem. Soc.* **1992**, *114*, 588.